Hocine BOUCHEKHOU[1], Mohamed Rachid MEKIDECHE[2], Jean LEVEQUE[3]

University of Jijel, Algeria (1, 2), University of Lorraine, France (3)

Torque simulation in a reluctance motor design incorporating HTS materials in both stator and rotor parts

Abstract. In this work, a fully high temperature superconducting reluctance motor (HTS RM) is studied. A smallest configuration of HTS armature winding based on the mechanical characteristics of HTS BSCCO tape is determined. Furthermore, a novel rotor topology of single HTS YBCO bulk with ferromagnetic material is proposed. Electromagnetic torque of HTS RM is calculated by finite element method (FEM) with 2D consideration. The characteristics of the bipolar HTS RM are compared with a conventional motor with HTS rotor.

Streszczenie. Opisano silnik reluktancyjny z elementami wykonanymi z wysokotemperaturowego nadprzewodnika. Do uzwojenia wykorzystano taśmę HTS BSCCO. Zaproponowano też nową konstrukcję wirnika z materiału HTS YBCO. Obliczono moment elektromagnetyczny wykorzystując metodę elementów skończonych. Symulacja momentu w silniku reluktancyjnym wykorzystującym nadprzewodnik HTS w stojanie i wirniku.

Introduction

Electrical machines have made significant progress through the development of HTS materials. Recently, several researches prove that the extern variables of the conventional machines are most important by considering HTS elements in the fixed or rotating part of machines [1-4]. The majority realized works related to superconducting reluctance motors is to increase the value of output power, efficiency and power factor at nitrogen liquid (77K) and at other low temperatures [5-8]. Most reluctance motors adopt HTS elements in the rotor by replacement of the non-magnetic regions with HTS bulk elements, in which bulks had the property to expulse the entire field lines from material surfaces (Meissner effect). The HTS rotors present different topologies known as Zebra, Zelz and Pilz types [9]. Despite of the improvements that present these topologies in the output characteristics of the motor, restrictions are due to limitation of the applied current in the copper stator windings which limit the output power.

To increase the applied current in armature winding, a team of researchers cooled completely a motor with copper stator and HTS rotor by immersion in nitrogen liquid [10]. Despite of the four times increase in the applied current, this value remains not enough to satisfy the expected purposes for high power motors.

In a conventional synchronous motor, copper wires were replaced by HTS MgB2 in both stator and rotor [11]. Otherwise, a racetrack pancake coils with YBCO tape in stator was adopted for a squirrel-cage induction motor [12].

In order to maximize power and torque with reducing volume, we proposed a novel design for a fully HTS synchronous reluctance motor. The armature winding consists of three racetrack shape concentric coils with HTS BSCCO tape however the rotor is composed of a single HTS YBCO bulk with ferromagnetic material. Our focus in this paper is to simulate the torque in order to evaluate the proposed design.

Regions Characteristics of HTS RM Design

In geometric model of fully HTS RM, two kinds of superconductors materials are used in the stator and rotor parts of the motor (Fig. 1). In the stator part, a simple structure of a three-phase concentric HTS winding is considered for generating a rotating magnetic field in the motor air gap. Field coils are designed with HTS BSCCO tapes where an AC current is applied in each phase coil ((A-A'), (B-B') and (C-C')). Such HTS coils are placed in a non-magnetic material (glass fiber material), represented in region II. In the rotor, a single HTS bulk of YBCO material (region IV) placed in a ferromagnetic cylinder (region III). The fully HTS RM configuration presents a small air gap between region II and III (gray area in Fig.1).

A stator yoke (region I), acting as a magnetic shield, is placed in the outer diameter of the superconducting armature winding. The proposed fully HTS RM is externally cooled by complete immersion of the motor in the nitrogen liquid at 77 K. The cooling system allowed us to consider a low thickness air gap. The geometrical parameters (α, β and γ) as shown in Fig. 1 stand for the slot opening angle , the minimum opening angle of the coil and the angle corresponding to the HTS bulk thickness respectively.
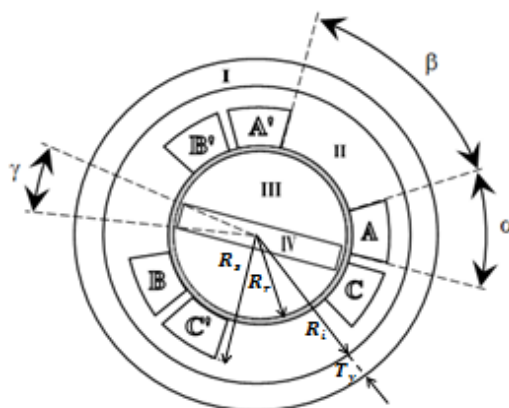

Fig 1. Cross-sectional view of fully HTS RM.

Sizing steps of HTS coil with BSCCO tape

Not all known winding configurations realized by HTS BSCCO tapes are possible; a concentric winding shape is well adapted due to the mechanical characteristics of HTS tapes. Stator winding is consisted of three identical coils (A-A'), (B-B') and (C-C') shifted with the same electrical angle (120 degree). Table 1 gives specifications of the HTS BSCCO type candidate produced by Sumitomo Electric (type H) and American superconductor Corp [13-14].

To ensure mechanical bending strength of HTS BSCCO coils, we have chosen for our simulation a bending radius of 40 mm. According to this choice, dimensions of the stator coils have been conceived by considering a minimum opening angle. The value of the angle α is directly related to specific parameters of BSCCO tape (width and thickness) and choice of global coil size.

Tape parameters	Values
Width [mm]	4.26
Thickness [mm]	0.28
Critical current I_c at 77K, self field [A]	150
Critical bend diameter [mm]	40

Stator topology with HTS coils

Technically, it is not feasible to occupy the entire trapezoidal section of the stator slot with the rectangular cross-section of HTS BSCCO coil (see Fig. 1). To give solution to this problem, a rectangular form of the slot is proposed in Fig. 2(a), where four sub-coils of thickness *w* are stacked along the y-axis, this *w* parameter is also the width of BSCCO tape. Each sub-coil is composed of ($n \times d$) distance of along the x-axis where *d* and *n* are respectively the thickness and the number of turns of BSCCO tape. The slot cross section represented in Fig. 1 is subdivided into three sections; a rectangular one in which HTS tapes are placed and two other identical triangular sections considered from glass fiber. The HTS phase coil represented in Fig. 2(b) has a racetrack-shape with four layers. Each sub-coil (layer) is composed of *n* parallel face-to-face stacked tapes to guarantee a sufficient carrying current. The length *L* is the straight portion of the HTS coil or the active part of HTS RM along the z-axis and *R* is the bend radius of the coil (Table 1). The aim of this step is to concept a smallest possible configuration of stator by using HTS BSCCO tape characteristics in order to increase the applied current density in the armature winding. Therefore, reducing the volume compared to stators of other motors with the same output power.
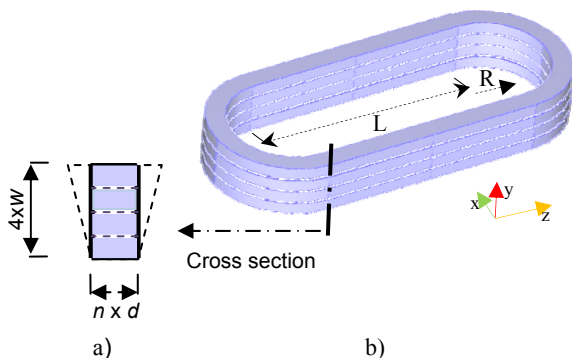

Fig 2. Sketch of racetrack-shape HTS phase coil: (a) cross section of stator slot and (b) HTS coil structure.

Rotor topology with HTS Bulk

Generally, the rotor of conventional reluctance motors is compound with magnetic and non-magnetic materials. Therefore, two inductances are considered along the direct and quadrature-axis (L_D and L_Q). In Fig. 3, the difference between L_D and L_Q ($L_D - L_Q$) affects the electromagnetic torque. It is possible to rise the reluctance torque with increasing the flux density along the D-axis or decreasing it along the Q-axis. We have envisaged a new topology by placing a perfect diamagnetic HTS YBCO bulk in the rotor structure. This superconducting element (YBCO) has to exclude the perpendicular field over the total axial length (z-axis). Then, the flux density is concentrated in the D-axis and permits a minimum inductance in Q-axis. The rotor topology shown in Fig. 3 consists of an HTS YBCO bulk with a rectangular section ($l \times e = 42 \times 8 \ mm^2$) placed in a ferromagnetic cylindrical structure along the z-axis. To maintain the HTS bulk in its region, two ferromagnetic cylinders of short length (in the z-axis) are fixed on the borders of the rotor. This structure is very advantageous, since it allows a good protection of HTS Bulk, simple to build and robust.
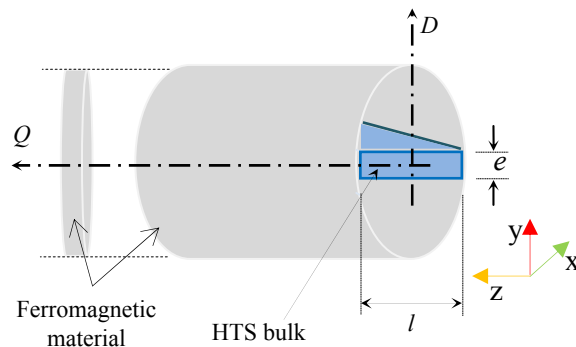

Fig 3. Rotor topology with HTS bulk.

HTS RM Model Simulation
Numerical Model of HTS Motor

The fully HTS RM configuration is composed of a bipolar HTS stator winding and a HTS bulk in the rotor. To evaluate the potential performance of the motor, a numerical study has been developed using FEMM Software [15].

Table 2 gives geometrical parameters of the two dimensional (2D) model of HTS RM. Different assumptions have been considered in the 2D calculation model. First, The HTS motor is supposed infinitely long according to z-axis direction (see Fig. 2 and 3). Consequently, the end effects are neglected. Furthermore, all the used ferromagnetic material is supposed linear, and possesses a constant and high value of relative permeability ($\mu_r \gg 1$). This assumption is related to neglecting material saturation which induces hysteresis losses that affect negatively power and torque values. We also consider that the HTS bulk rotor has a perfect diamagnetic behavior, so a low relative permeability is requested for this material ($\mu_r \ll 1$). Finally, the magnetic permeability of region II in the stator is taken equal to air permeability. A three-phase sinusoidal current is applied to the HTS coils of the stator with a frequency of 50 Hz and current value of 95 A.

Table 2. Geometrical Parameters of HTS RM.

Motor parameters	Values
Back iron thickness (T_y)	20 mm
Stator inner radius (R_i)	45 mm
Stator outer radius ($R_i + T_y$)	75 mm
Rotor radius (R_r)	43 mm
Slot radius (R_s)	65 mm
Air gap thickness	02 mm
Depth of motor	360 mm
α	27.5 deg
β	60 deg
γ	20 deg

The concentric shape of the HTS stator coils is more suitable for the HTS BSCCO tape characteristics. This configuration is easy to manipulate and can carry significant current densities but this structure generally causes vibrations due to significant generated torque ripples [16]. A parametric study with the FEMM software was considered in order to achieve a final structure of rotor with minimum ripples. So, the size and the number of HTS bulks in the rotor are not randomly chosen but they are determined numerically to have the suitable size giving the minimum ripples and the maximum torque value.

In our simulation, three rotor topologies are taken into account:

- The first case is a ferromagnetic structure with HTS YBCO, (YBCO-Fer) topology as shown in Fig. 3.

- The second case, HTS YBCO is replaced by an air core, (Air-Fer) topology.
- In the last case, the ferromagnetic cylinder is replaced with the air core, (YBCO-Air) topology.

Numerical Results

The fully motor structure is represented in the following figure (Fig. 4). A triangular finite element mesh is used to solve the 2D problem.

In fig. 5, the two poles of the machine are represented by the distribution of the magnetic field lines. We observed that the superconducting bulk in the rotor prevents all the penetrations of flux lines in its region corresponding to its perfect diamagnetic behavior considered in this simulation (low magnetic permeability is proposed).
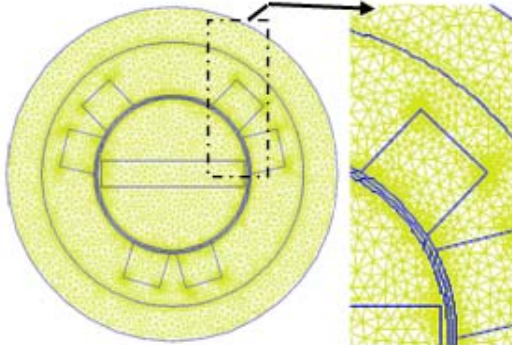
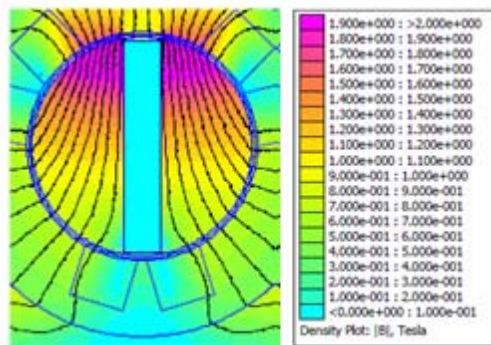

Fig 4. 2D FEM mesh for the HTS RM

Fig 5. Magnetic field distribution in a cross-section of motor structure

The FEMM software uses Maxwell stress tensor for calculating electric and magnetic forces, based on the Lorentz force density. It applies the divergence theorem to convert the volume integral to a surface integral. The torque is calculated from the local distribution of magnetic force [17].

The FEM simulation is realized for three different structures of rotor. Figure 6 shows the variations of the static torque versus the rotor position of the HTS motor. Ferromagnetic rotor with bulk HTS (YBCO-Fe) has a maximum value of the static torque (635 Nm) and the rotor topology without HTS material (YBCO replaced by Air core) that presents a low torque value of 120 Nm. So, we observe an increased torque value of more than five times for the (YBCO-Fer) topology compared to the (Air-Fer) one. This gain of torque is inherent to HTS YBCO bulk characteristics used in the rotor configuration. Also, the (YBCO-Fer) rotor topology presents about a double value of torque compared to the rotor without ferromagnetic material (YBCO-Air) (300 Nm only). This result is due to the magnetic permeability of ferromagnetic material.
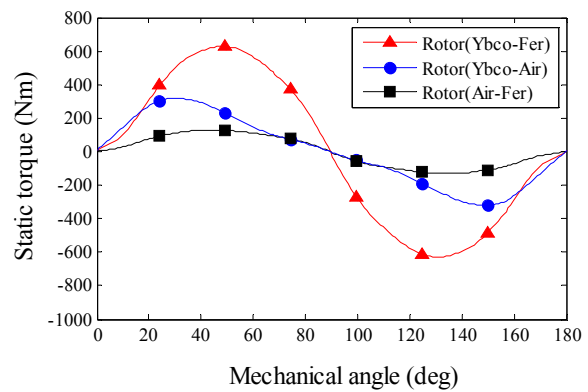

Fig 6. Static torque according to a mechanical angle for different rotor topologies: (YBCO-Fe), (YBCO-Air) and (Air-Fe).

The variation of the dynamic torque as a function of rotor position in the HTS motor is shown in Fig. 7. The (YBCO-Fer) topology of HTS rotor has been adopted for the calculation of this torque. The average torque value of 608 Nm with a ripple torque of 3.5% has been obtained by the FEMM simulation. A similar value of torque was generated previously [10] for a greater size motor with HTS rotor. This confirms the aim of our work to create small sized motor with an important torque value and weak ripples of torque.
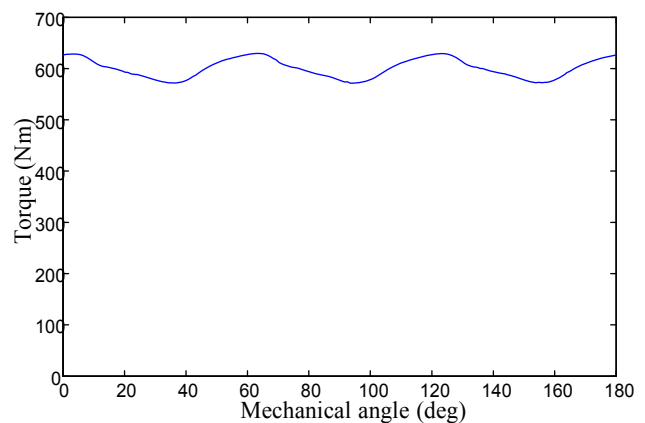

Fig 7. Torque versus rotor position.

In table 3, we observe decreasing values of maximal torque with the increase of air gap thickness. A 645 Nm is obtained with 1 mm but only 571 Nm with a thickness of 5 mm. We have even presented the maximal values of the output power according to the air gap thickness, calculated using the following formula:

$$(1) \qquad P = C \times \omega$$

where: P – output power (W); C – electromagnetic torque (Nm); Ω – rotation speed of the motor (rd/s).

$$(2) \qquad \omega = \frac{2\pi f}{p}$$

where: p– number of pairs of poles; f – applied current frequency.

Table 3. Maximal torque and power values versus air gap thickness.

Designation	Values				
Air gap thickness [mm]	1	2	3	4	5
Maximal torque [Nm]	645	635	610	591	571
Maximal power [KW]	202	199.3	191	185	179

The advantage of the used cooling system for our HTS motor design (cooling with nitrogen liquid) allowed us to adopt a low thickness of the air gap. Since the use of the

cooling cryostat around the HTS rotor requires an increase of the air gap thickness which causes a decrease of the torque value. In our motor, the air gap thickness is chosen at 02 mm for the reason to compare the output power with another HTS motor having the same air gap. According to the values reported in table 3, the output power of our HTS RM is 199.4 kW at 3000 rpm. This last power value observed is practically the same one achieved with the HTS reluctance motor at copper stator and HTS rotor (200 kW) tested in [10] at 50Hz and 77K, But our fully HTS design present a reduction of volume more than two times (2.3 times). The advantage of our HTS RM is that it produces an important power with a compact size, due to the high current applied in the HTS stator winding and the perfect characteristics of HTS bulk. Furthermore, the rotor HTS topology presents simplicity for possible realization and a good mechanical protection for the HTS bulk.

Approximation of AC losses

Under these operating conditions (50Hz and 77K), we have presented an approximation of AC losses. The total AC losses are composed from the magnetization losses caused by the perpendicular field on the windings (greater part of losses) and transport losses generated by the AC current applied in the HTS windings. In our motor, each stator coil presents about 280 m of BSCCO tape length. As reported in [18], the approximation of total losses power for one coil is 282.8 W. Consequently, the total AC losses for the three coils are 848.4 W. AC losses are estimated with a ratio of 0.4% on the output power of the HTS RM.

Conclusion

In this paper, a fully superconducting reluctance motor has been modeled by 2D finite element method (FEM). The proposed HTS RM design has given us an important torque value with a low ripple.

Using HTS materials in both stator and rotor parts has reduced the total volume up to half compared to a conventional motor having the same output power (200 kW) with just HTS material in rotor. So, this novel HTS design allows producing more compact motors.

Concentric winding form facilitates stator structure conception and requires less material and cost compared to distributed winding one. In addition, the presence of the magnetic screen with ferromagnetic material (YBCO-Fer) in the rotor topology has increased twice as much the torque value compared to the topology with just HTS material (YBCO-Air) and offers good mechanical protection for HTS bulk.

The proposed fully HTS RM with less air gap thickness can achieve higher powers if we overcome size limits handicap of the available bulks.

Authors: *Hocine Bouchekhou. University of Jijel, Faculty of science and Technology, L2EI Laboratory, B.P 98 Ouled Aissa Jijel, Algeria, E-mail:* hbouchekhou@gmail.com ;
Mohamed Rachid Mekideche. University of Jijel, Faculty of Science and Technology, L2EI Laboratory, B.P 98 Ouled Aissa Jijel, Algeria, E-mail: mek_moh@yahoo.fr ;
Jean Lévêque. University of Lorraine, Faculty of Sciences and Technologies, GREEN Laboratory, France, E-mail: jean.leveque@univ-lorraine.fr

REFERENCES

[1] Feng Lin, Rong Hai Qu and Da Wei Li, "Topologies for fully superconducting machines", Proceedings of IEEE International Conference on Applied Superconductivity and Electromagnetic Devises (ASEMD)", Shanghai, China, November.20-23, 2015.

[2] Mark Ainslie, Mitsuru Izumi and Motohiro Miki, "Recent advances in superconducting rotating machines: an introduction to the Focus on Superconducting Rotating Machines", Superconductor Science and Technology, Vol. 29, No. 6, id.060303, 2016.

[3] K. S. Haran, S. Kalsi, T. Arndt, H. karmaker, R. Badcock, B. Buckley, T. Haugan, M. Izumi, D. Loder, J. W. Bray, P. Masson and E. W. Stautner, "High power density superconducting rotating machines-Development status and technology roadmap", Superconductor Science and Technology, Vol. 30, No. 12, id.123002, 2017.

[4] K. Kovalev, N. Ivanov, I. Kobzeva, E. Tulinova, "High specific power HTS eclectic machines", PRZEGLAD ELEKTROTECHNICZNY, Volume 93, Issue 11, 2017, pages 125-128.

[5] L. K. Kovalev, K. V. Ilushin, K. L. Kovalev, V. T. Penkin, V. N. Poltavets, S. M-A. Koneev, I. I. Akimov, W. Gawalek, B. Oswald and G. Krabbes, "High output power of eclectic motors with bulks HTS elements", Physica C: superconductivity, Vol. 386, 419-423, 2003.

[6] S. D. Chu, and S. Torii, "Torque-speed characteristics of superconducting synchronous reluctance motors with DyBCO bulk in the rotor", IEEE transactions on applied superconductivity, Vol. 15, No. 2, 2178-2181, 2005.

[7] M. Qiu, Z. Xu, Z. H. Yao, D. Xia, L. Z. Lin, G. M. Zhang, L. Xiao, H. T. Ren, Y. L. Jiao and M. H. Zheng, "Design and performance of a small HTS bulk reluctance motor", IEEE transactions on applied superconductivity, Vol. 15, No. 2, 1480-1483, 2005.

[8] A. L. Rodrigues, and A. J. Pires, "Reluctance machines incorporating high temperature superconducting materials on the rotor", Physica C: Superconductivity, Vol. 470, No. 2, 98-103, 2010.

[9] L. K. Kovalev, K. V. Ilushin, V. T. Penkin, K. L. Kovalev, A. E. Larionoff, S. M-A. Koneev, K. A. Modestov, S. A. Larionoff, V. N. Poltavets, I. I. Akimov, V. V. Alexandrov, W. Gawalek, B. Oswald and G. Krabbes, "High output power reluctance electric motors with bulk high-temperature superconductor elements", Superconductor Science and Technology, Vol. 15, No. 5, 817-822, 2002.

[10] B. Oswald, K. J. Best, M. Setzer, M. Söll, W. Gawalek, A. Gutt, L. Kovalev, G. Krabbes, L. Fisher and H. C. Freyhardt, "Reluctance motors with bulk HTS material", Superconductor Science and Technology, Vol. 18, No. 2, S24-S29, 2004.

[11] K. Kajikawa, Y. Uchida, M. Hosseina, T. Nakamura, H. Kobayashi, T. Wakuda and K. Tanaka, "Development of Stator Windings for Fully Superconducting Motor With MgB2 Wires", IEEE Transactions on Applied Superconductivity, Vol. 23, No. 3, 5201604-5201604, 2013.

[12] B. Liu, R. Badcock, H. Shu and J. Fang, "A Superconducting Induction Motor with a High Temperature Superconducting Armature: Electromagnetic Theory, Design and Analysis", Energies, Vol. 11, No. 4, 792-792, 2018.

[13] N. Ayai, S. obayashi, M. Kikuchi, T. Ishida, J. Fujikami, K. Yamazaki, S. Yamade, K. Tatamidani, K. Hayashi, K. Sato, H. Kitaguchi, H. Kamakura, K. Osamura, J. Shimoyama, H. Kamijyo and Y. Fukumoto "Progress in performance of DI-BSCCO family", Physica C: Superconductivity, Vol. 468, No. 15-20, 1747-1752, 2008.

[14] N. K. Paramoda, U. Prasad, A. Amardas, D. Patel and S. Pradhan, "Design and fabrication of a high Tc BSCCO based square helmholtz coil", Journal of Physics: Conference Series, Vol. 208, No. 1, 012021, 2010.

[15] D. Meeker, "Finite element method magnetics: User's Manual", version 4.2 , Octobre 2015.

[16] J. Min Park, S. Il Kim , J. Pyo Hong and J. Ho Lee, "Rotor design on torque ripple reduction for a synchronous reluctance motor with concentrated winding using response surface methodology", IEEE Transactions on Magnetics, Vol. 42, No. 10, 3479-3481, 2006.

[17] S. McFee, J.P. Webb and D.A. Lowther, "A tunable volume integration formulation for force calculation in finite-element based computational m agnetostatics", IEEE transactions on magnetics, Vol. 24, No.1, 439-440, 1988.

[18] S. Stavrev, F. Grilli, B. Dutoit and S. P Ashworth, "Comparison of the AC losses of BSCCO and YBCO conductors by means of numerical analysis", Superconductor Science and Technology, Vol. 18, No. 10, 1300-1312, 2005.